

# Development of Low-cost Deformation-based Micro surface texturing system for Friction Reduction

Song Xu<sup>1,2#</sup>, Sam Oh Jin An<sup>1,2</sup>, Danno Atsushi<sup>1</sup> and Sylvie Castagne<sup>2</sup>

<sup>1</sup> Singapore Institute of Manufacturing Technology (SIMTech), 71 Nanyang Drive, Singapore, 638075  
<sup>2</sup> School of Mechanical and Aerospace Engineering, Nanyang Technological University, Singapore, 639798  
# Corresponding Author / E-mail: songx02@gmail.com, TEL: +65-6793-8595, FAX: +65-6791-6377

KEYWORDS : Micro surface texturing, micro incremental embossing, hydrodynamic lubrication, boundary lubrication, friction

*Surface texturing as a means for enhancing tribological properties of mechanical components has been under intensive investigation over the last two decades. Many methods have been proposed to create surface texture of various patterns and geometries. However, among all these methods, deformation-based micro-surface texturing is least studied. It has many advantages over other methods that could lead to immediate industry application, including high productivity, high geometry fidelity and low cost. In the current work, a simple but effective incremental micro embossing system based on a commercially available press has been developed to create micro surface textures of various shapes and depths with accuracy up to 5µm. The friction coefficients of the textured surfaces have been tested at different loadings and speeds with various lubricants to demonstrate their friction reduction capability. It has been observed that at high speed conditions, the friction reduction is achieved by the hydrodynamic lift. Interestingly, at the low speed conditions, the micro-surface texture is still capable of reducing the friction, thanks to its lubricant retention and debris entrapment capability. A micro surface textured mechanical face seal demonstrator has been built to further evaluate the micro surface texture created by incremental embossing method. A reduction of 20% in torque friction has been consistently achieved, which is on a par with that of the laser surface texturing method.*

Manuscript received: August XX, 201X / Accepted: August XX, 201X

## 1. Introduction

The application of surface texturing for tribology improvement attracts special attention, as this is the most cost-effective way for energy consumption reduction as mentioned by Bruzzone et al<sup>1</sup>. By having a controlled texture on one of two faces in relative motion, it provides many positive effects, such as reduction of friction and wear, and increase in load capacity. Early studies by Hamilton et al.<sup>2</sup> and Anno et al.<sup>3,4</sup> recognized the potential of micro-asperities to provide hydrodynamic lift during film lubrication, while later research by Tian et al.<sup>5</sup> indicated that small-scale texturing could also provide lubricant reservoirs in poorly lubricated conditions and trap wear particles in boundary and dry lubrication. A further use of micro-textured surfaces was found by Tonder<sup>6</sup> in the use of partial texturing – a textured region can take the place of macro-geometry such as steps or inclined planes meant to provide hydrodynamic lift. Research and analysis presented to date demonstrate both the potential to improve tribological properties via surface texturing, and the need to understand the materials, lubricants, and operating

conditions before a surface texture can be applied.

Micron-scale surface textures were not limited to grooves and troughs, but also complex patterns of different shapes, including circular, triangular, and other geometric shapes, to be used<sup>1</sup>. Asperity shape, area, depth, area ratio (the ratio of asperity to flat area) and orientation can all impact the effectiveness of a given texture as discussed by Han et al.<sup>7</sup> through CFD simulation. Nowadays, many manufacturing techniques are available to create surface features with sizes and accuracy in the micrometer range. Techniques such as micro-machining used by Greco et al.<sup>8</sup>, Brinksmeier et al.<sup>9</sup> and Graham et al.<sup>10</sup>, micro-EDM used by Byun et al.<sup>11</sup>, and laser surface texturing (LST) used by Etsion et al.<sup>12-18</sup> are the most explored, thanks to their versatility and ease of implementation. However, they are still not widely implemented in the industry due to the intrinsic problem of its low throughput, as the dimples on the surface have to be created individually<sup>19</sup>. For laser surface texturing, the heat-induced shape distortion (feature fidelity and geometry/position accuracy) is another major drawback. Cao et al.<sup>20</sup> introduced a desktop-size deformation-based surface

texturing system which resembles a micro rolling mill. It is able to produce micro features of tens of microns on sheet materials with high throughput and smooth surface. It has good potential for industry application in micro heat exchanger and friction reduction. However, only sheet materials can be produced in such instance. On the other hand, using embossing method for deformation-based micro surface texturing can be a powerful alternative, as it applies to both sheet and bulk materials, which were presented by Pettersson and Jacobson<sup>21,22</sup>. Even-size dimples can be produced over areas up to  $78.5 \text{ mm}^2$  in a single punch, which makes it very fast and productive. Therefore, it is naturally the focus of the current study. In the current work, a low-cost incremental micro embossing system has been developed to create micro surface textures of various shape and depths on the component with overall accuracy up to  $5 \text{ }\mu\text{m}$  using a commercially available press. Such setup includes an in-house constructed high load bearing XY stage, which allows accurate positioning of the workpiece to form the surface texture locally or in large area by incremental steps. This gives more flexibility to the embossing process as more complex geometry workpiece can be textured. The friction coefficients of the textured surfaces have been tested at different loadings, lubricants and speeds to demonstrate their friction reduction capability. Furthermore, a micro surface textured mechanical face seal demonstrator has been built to further evaluate the effectiveness of the texturing method in operation. A reduction of  $\sim 20\%$  in friction torque has been consistently achieved, on par with that using the laser surface texturing method.

## 2. Experimental procedures

### 2.1 Setup of a low-cost incremental micro embossing system

The setup of the low-cost incremental micro-embossing system is based on the Schmidt ServoPress Type 420. It has a displacement-control resolution of  $10 \text{ }\mu\text{m}$  and load-control resolution of  $100 \text{ N}$ , which is among the average accuracy in the Schmidt ServoPress product family. To achieve a required accuracy of  $5 \text{ }\mu\text{m}$  over a large area for friction reduction application, the load control mode is selected. Because of the low rigidity of the C-shape press and low displacement resolution ( $10 \text{ }\mu\text{m}$ ), displacement control is not a good option for open-die embossing. Load control is chosen with a large punch area, as that will give higher load increment with the same embossing feature depth.

The top punches are made of D2 tool steel with head dimension  $3 \times 3 \text{ mm}$ . It has  $15 \times 15$  uniform protrusions with height  $40 \text{ }\mu\text{m}$ , pitch  $200 \text{ }\mu\text{m}$  and tapering angle  $15^\circ$ . There were two punches used in this study, one with square shape feature of side length  $100 \text{ }\mu\text{m}$  and the other with circular shape feature of diameter  $100 \text{ }\mu\text{m}$ . Such features are wire-EDM (Electric Discharge Machining) cut to a tolerance of  $2 \text{ }\mu\text{m}$  from a standard shoulder punch component provided by MISUMI Inc. Fig. 1(a) illustrates the surface profile of the punch with circular feature under 3D contactless optical microscope. A line profile of the micro protrusions is provided in Fig. 1(b).

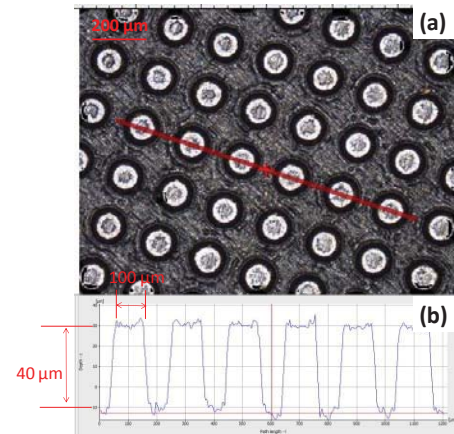


Fig. 1 (a) 3D Optical micrograph of the male textured punch (round feature); (b) Line profile of the protrusions on the punch head

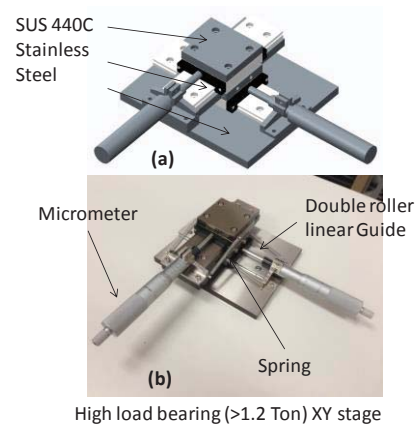


Fig. 2 Illustration of the (a) design and (b) assembly of the high accuracy, high load bearing XY stage used in the micro embossing study

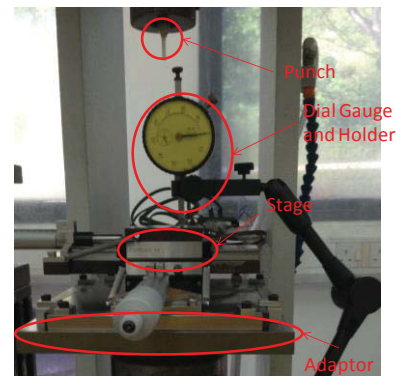


Fig. 3. Setup for the XY stage alignment inspection

The bottom die consists of an in-house constructed XY stage with  $1 \text{ }\mu\text{m}$  resolution and  $50 \text{ mm}$  travel, which is tailored for high-load bearing usage ( $>1.2 \text{ Ton}$ ) such as embossing. Miniature high load rating linear guides are used for the stage movement with static load up to  $14.3 \text{ kN}$  and accuracy  $\pm 0.5 \text{ }\mu\text{m}$ . The stage movement is micrometer controlled and spring-loaded to maintain accurate positioning with easy modification for upgrade to motorized control. All the load-bearing plates are made of SUS 440C Martensitic Stainless Steel harden by sub-zero treatment, the same as the slides, to maintain high hardness ( $56 \text{ HRC}$ ) and good flatness (grinding to  $< 0.1 \text{ }\mu\text{m}$ ). Fig. 2 illustrates the design and assembly of the XY

DOI: XXX-XXX-XXXX

stage used in the current study. With such stage, the workpiece can be moved freely to allow partial or full embossing of the surface. Such accuracy cannot be easily/economically achieved using the moving punch configuration as it requires high rigidity of the entire press frame. The XY stage was then mounted on the lower stand through an adapter, the accuracy of the entire setup was inspected by a micron dial gauge, which is illustrated in Fig. 3. The alignment accuracy of the entire setup can be maintained within  $\pm 1 \mu\text{m}$ .

## 2.2 Friction test setup

The friction tests were carried out using a CETR-UMT multifunctional tribometer with pin-on-pad configuration for low speed testing (Fig. 4(a)) and pin-on-disc configuration for high speed testing (Fig. 4(b)). The mating stainless steel SS316L counterparts are fully immersed in the commercially available oil during all the tests. Two types of lubricants were tested separately: SAE 30 (viscosity 0.31 Pa·s) and Ultima (mainly vegetable oil, viscosity 0.05 Pa·s).

The top pin of sizes 3 mm (pin-on-pad) and 12 mm (pin-on-disc) in diameter was used. The surfaces of the mating counterparts were polished to mirror finish, and two types of surface textures (round and square dimples) with 4 different depths of dimples (0  $\mu\text{m}$ , 10  $\mu\text{m}$ , 20  $\mu\text{m}$  and 30  $\mu\text{m}$ ) were punched onto the lower pad/disk using our low-cost micro embossing system with additional lapping to the roughness of  $R_a = 0.01 \mu\text{m}$ . Five different load conditions were applied during the tests: 0.5 kg, 1 kg, 2 kg, 4 kg and 8 kg, which corresponds to  $\sim 100$ -1600 psi in pin-on-pad configuration and  $\sim 6$ -100 psi in pin-on-disc configuration.

Various speeds ranging from 0.1 mm/s for pin-on-pad to 50~500 mm/s for pin-on-disc were chosen to ensure different lubrication conditions are tested (boundary, mix and hydrodynamic lubrications). Various loadings applied further ensure such assumption. For the low speed (0.1 mm/s), high loading (1600 psi) combination, it is arguably close to that of the engine start/stop condition where boundary lubrication dominates. For the high speed (500 mm/s), low loading (6 psi) combination, it is close to the stable mechanical seal operating condition (1000 mm/s and 30 psi) where hydrodynamic lubrication prevails.

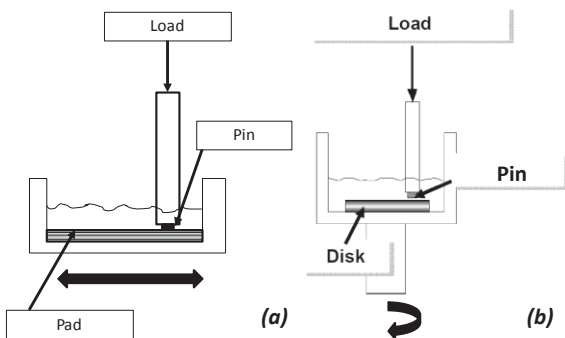


Fig. 4. (a) Pin-on-pad configuration for low speed coefficient of friction testing and (b) Pin-on-disc configuration for high speed coefficient of friction testing

## 3. Results and Discussions

### 3.1 Surface texture profiles

Examples of the resulting surface texture profiles manufactured by the current low-cost micro embossing setup are illustrated in Fig. 5. Regular round and square dimple arrays with various depths can be embossed on the surface as well as patterns such as the word “SIMTech”. The dimple depth control is achieved through control of the loading force. By applying different forces on the sample, different dimple depths can be achieved. The depths were determined using Alicona optical microscope, which allows obtaining the entire 3D profile of the dimples and hence measuring their depths. Fig. 5d shows Alicona micrograph of round dimple pattern cross section along the sampling line with depth of  $17.5 \pm 2 \mu\text{m}$  created by 6kN loading force and Fig. 5e shows micrograph of round dimple pattern cross section along the sampling line with depth of  $29.5 \pm 2 \mu\text{m}$  created by 8kN loading force. Based on this approach, the relationship between the loading force and the dimple depth can be found and a reference chart for stainless steel SS316L can be produced. From the chart, the theoretical load-control depth resolution can be calculated as  $0.5 \mu\text{m} = 5 \mu\text{m}/1000 \text{ N} * 100 \text{ N}$  (load resolution). However, it is worth noting that the dimple depth over individual punch area is not uniform due to the small misalignment of the XY stage to the top punch. Considering this effect, together with the surface roughness of the punch, the actual overall system accuracy for embossing the dimples can only reach  $\approx 5 \mu\text{m}$ .

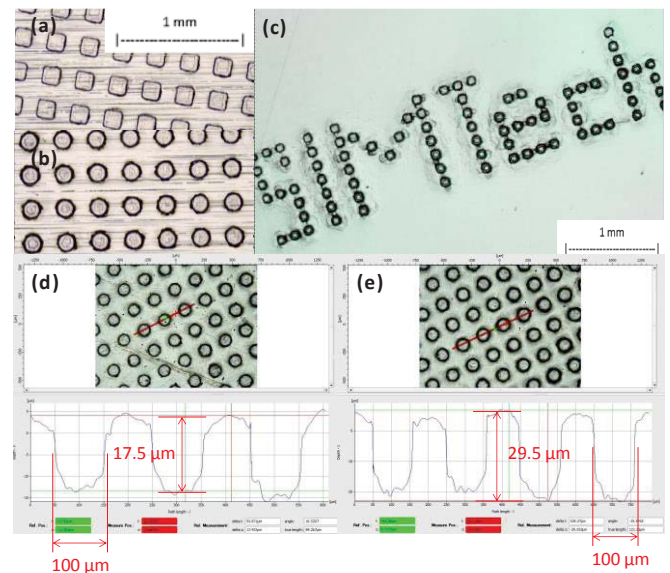


Fig 5. Alicona optical micrographs of the surface textures with (a) square (b) round (c) word “SIMTech” dimple patterns (d) Round dimple pattern cross section along the red sampling line with depth 17.5  $\mu\text{m}$  created by 6kN loading force (e) Round dimple pattern cross section along the red sampling line with depth 29.5  $\mu\text{m}$  created by 8kN loading force

3.2 Friction test results

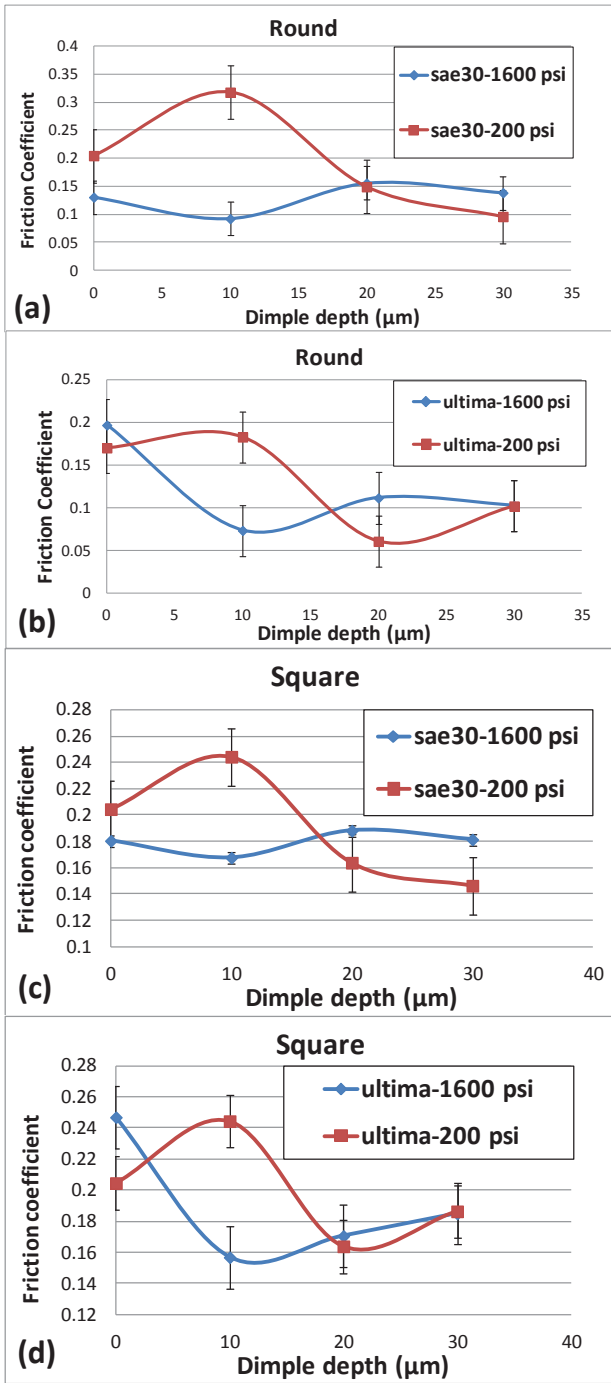


Fig. 6. Plots of the friction coefficients under different pressures for different dimple depths and geometries (round and square) using two types of lubricants in low speed test

For the low speed (0.1 mm/s) pin-on-pad test, the effect of the pressure on the optimal dimple depth is plotted in Fig. 6. For two different types of lubricants and different dimple geometries, all have demonstrated that the optimal depth increases with decreasing pressure. The optimal dimple depth for SAE 30 under 1600 psi pressure is 10 μm for both round and square dimple patterns, while

it increases to 30 μm when the pressure drops to 200 psi. For low viscosity Ultima, the optimal dimple depth increases from 10 μm to 20 μm when the pressure decreases from 1600 psi to 200 psi. It is interesting to note that such observation coincides with the simulation results that Ma and Zhu<sup>23</sup> have previously presented, which was the case under hydrodynamic lubrication. Now similar observation is obtained under boundary lubrication. This may be due to the fact that micro-dimples, as lubricant reservoirs, help to retain and disperse lubricant during relative motion (even at low speed and high pressure), which transforms the dry boundary friction condition with flat surfaces into mixed friction condition with dimpled surfaces. Further confirmation comes from the fact that the dimple geometries (round and square) do not alter to the optimal dimple depth value, which can only happen in the dry and boundary friction condition, as the debris entrapment does not depend on the shape of the dimple but volume of the dimple cavity (whether the cavity is large enough to contain all the debris). Therefore, the friction reduction realized in this case is a combined effect of both lubricant retention and debris entrapment of the micro-dimples.

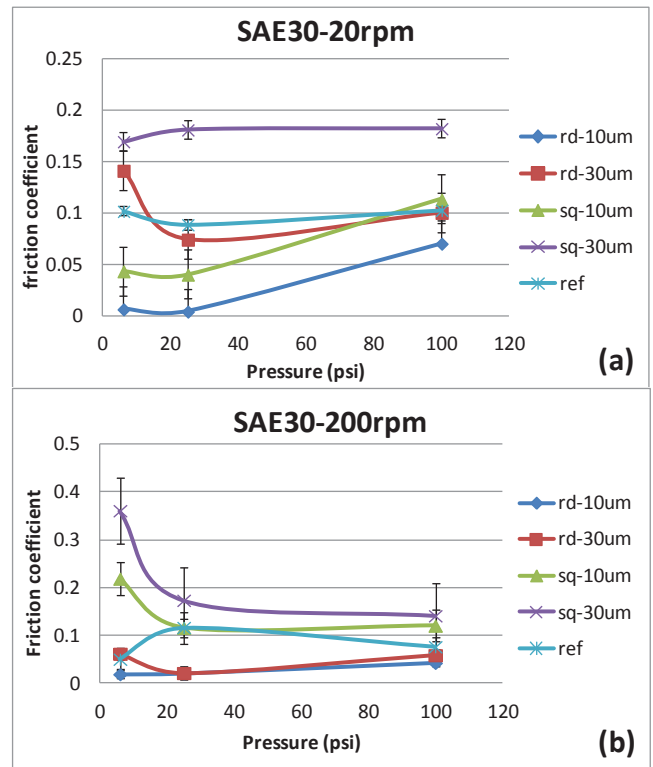


Fig. 7. Plots of the friction coefficients for round and square dimples at different depths using SAE30 lubricant at different pressures and speeds

For the high speed (50~500 mm/s) pin-on-disc test, again two types of lubricants were tested. Fig. 7 illustrates the dimple geometry, dimple depth and pressure effect on the friction when SAE30 is used. It can be clearly observed that, at different speeds (20 rpm angular speed corresponds to a line speed of 50 mm/s and 200 rpm corresponds 500 mm/s in the current experimental setup),

the reference flat surface gives an approximately constant friction coefficient of 0.1 irrespective of pressure. Friction reduction was best achieved (at least 30% reduction) by a combination of round dimple (20% area density) and 10  $\mu\text{m}$  depth (100  $\mu\text{m}$  diameter), which is very close to what Qiu<sup>24</sup> and Etsion<sup>25</sup> have reported. In contrast, the combination of square dimple and 30  $\mu\text{m}$  depth showed the detrimental effect of friction increment (at least 30% increase), which was the worst performer among all the tested conditions. Such observation can be explained by the hydrodynamic lubrication regime expansion theory proposed by Etsion et al.<sup>14</sup>. Micro dimples help to change the lubricant flow and increase the hydraulic lift between the mating counterparts, which splits the two components further apart and transform the mixed lubrication condition into hydrodynamic lubrication condition. However, if the dimples are too deep, the lubricant viscosity comes into play and increases the drag, hence increases the friction between the two parts. This explained why the round dimple with 30  $\mu\text{m}$  depth has worse performance than round dimple with 10  $\mu\text{m}$  depth. This was also true for the square dimple when comparing 30  $\mu\text{m}$  depth's result with 10  $\mu\text{m}$  one. For the same dimple shape and sliding speed, 10  $\mu\text{m}$  ones always show a lower friction coefficient. It is also worth noting that the pressure (although the operating pressure is set to be constant if a mechanical seal is considered) plays a role in the micro dimple friction reduction where 25 psi sees the lowest friction value.

illustrates the dimple geometry, dimple depth and pressure effect on the friction when Ultima was used as the testing lubricant. The reference flat surface gives an approximately constant friction coefficient of 0.1 at 200 rpm and 0.15 at 20 rpm. The combination of round dimple and 10  $\mu\text{m}$  depth (100  $\mu\text{m}$  diameter) again gave the best friction reduction (at least 30% reduction), while the square dimple 30  $\mu\text{m}$  depth remained the worst (at least no reduction). However the difference between the effect of round dimple 10  $\mu\text{m}$  depth and round dimple 30  $\mu\text{m}$  depth were diminishing due to low viscosity of the lubricant. For the same dimple shape and sliding speed, 10  $\mu\text{m}$  ones again showed lower friction coefficient than 30  $\mu\text{m}$ .

Based on the results above, it is shown that although there are huge variations in test conditions such as different lubricants, loads and speeds, the ranking of the dimples' effectiveness in friction reduction would not change (round 10  $\mu\text{m}$  was consistently the best, square 30  $\mu\text{m}$  was always the worst). Such "geometrical factors" seem to have a greater influence than the Stribeck ones (viscosity of the lubricant, load and speed) in the dimpled surface in comparison with the flat one. Moreover, no matter at high pressure low sliding speed or low pressure high sliding speed, the surface dimple texture always managed to reduce the friction significantly, sometimes up to 50% at the optimum dimple depth. However, such reduction attributes to different friction reduction mechanisms (lubricant retention and debris entrapment for the low Stribeck value and hydrodynamic lift for the high Stribeck value) at different lubrication conditions.

### 3.3 Design of a micro surface textured mechanical face seal demonstrator

In order to further validate the effectiveness of the micro surface texture created by the incremental embossing method, a mechanical face seal demonstrator has been designed and constructed, analogous to that of Xu et al.'s work<sup>26</sup>. The conceptual design is provided in Fig. 9. The lower seal ring (OD = 7 cm, ID = 5 cm) is the rotor, which is supported by the table and connected to the motor through coupling with speed up to 6000 rpm. The upper seal ring is the stator, which connects to the torque meter in order to obtain the torque during the operation. A vertical frame holds the torque meter and supports the motor.

Detailed demonstrator design can be determined based on the conceptual one by adding the torque meter holder and frame. A plastic container is glued together with the lower seal ring to contain the lubricant during the rotation. Additional dead weight of 4kg also was added on top of the static seal ring in order to ensure 30 psi contact pressure as in the industry standard. The detailed design and assembly is provided in Fig. 10.

During the tests, one of the lower seal rings was textured with round dimples of diameter 100  $\mu\text{m}$ , depth 10  $\mu\text{m}$  and area density of 20%, which was proven to be the optimal in the pin-on-disc test for SAE30 lubricant. The untextured seal ring is also used as the "control group". The demonstrator was firstly ramped-up from 600

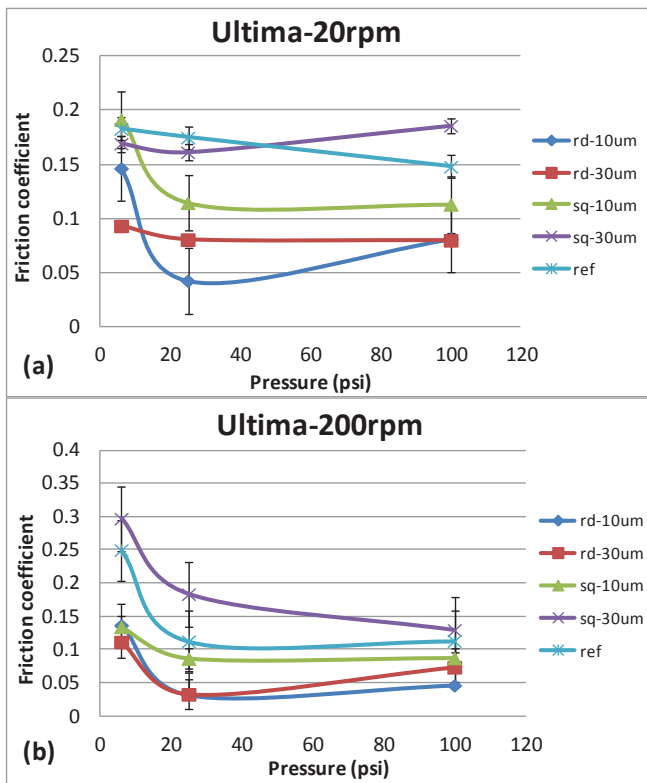


Fig. 8. Plots of the friction coefficients for round and square dimples at different depths using Ultima at different pressures and speeds

These findings are also applicable to Ultima case. Fig. 8

rpm to 2000 rpm in 2 minutes to simulate the engine start-up. The torque meter registered  $40 \pm 3$  Ncm and  $52 \pm 3$  Ncm net torque (reading with 4 kg load minus initial reading without 4 kg load) for textured and untextured rings respectively at 600 rpm and  $42 \pm 3$  Ncm and  $55 \pm 3$  Ncm net torque at 2000 rpm. A friction reduction of approximately 20% has been steadily achieved with micro surface texture at different speeds. Then, an endurance test of up to 2 hours at 2000 rpm has also been conducted on both rings to simulate the engine running at a constant speed scenario (i.e. car on the highway). There was no significant variation ( $\pm 3$  Ncm) of torque values observed in both cases, maintaining at 42 and 55 Ncm respectively. Visual inspection of the polished ring surfaces after the test found no visible scratch mark, indicating that at such speed, the lubrication condition is hydrodynamic and surface texture is effective in reducing the friction in the long run.

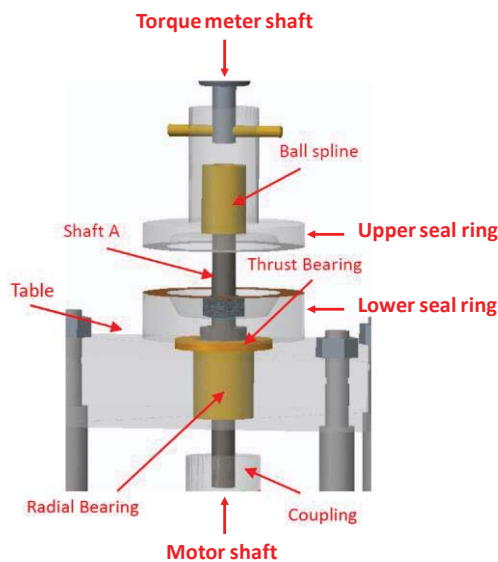


Fig. 9. Conceptual design of the mechanical face seal demonstrator core area: seal rings, bearings and shafts

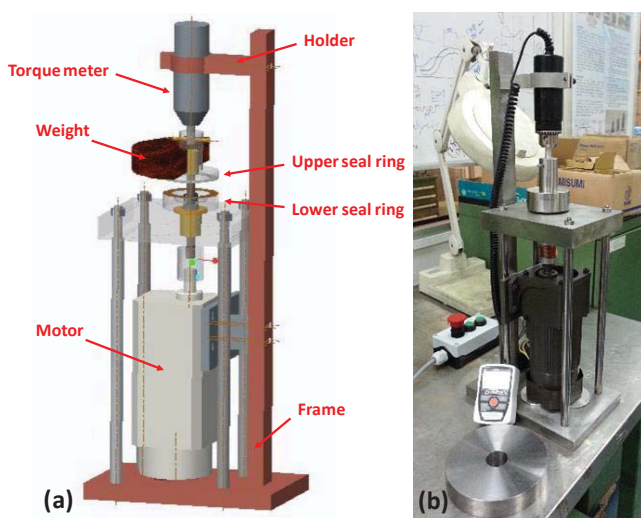


Fig. 10. (a) Detailed design and (b) Assembly of the mechanical face seal demonstrator with weight

#### 4. Conclusions

In the current study, a low-cost deformation-based incremental embossing system based on a commercially available press has been developed to create micro-surface textures of various shapes and depths with accuracy up to  $5\mu\text{m}$ . The friction coefficients of the textured surfaces have been tested at different loadings, speeds and lubricants to demonstrate their friction reduction capability. It has been observed that at both the low speed high load and high speed low load conditions, the micro surface texture is capable to reduce the friction significantly. However, such reduction attributes to different friction reduction mechanisms: lubricant retention and debris entrapment for the low Stribeck value condition and hydrodynamic lift for the high Stribeck value condition. A micro surface textured mechanical face seal rig has also been built to further demonstrate its capability in the operation.

#### REFERENCES

1. Bruzzone A.A.G., Costa H.L., Lonardo P.M. and Lucca D.A. "Advances in engineered surfaces for functional performance", CIRP Ann. Manuf. Technol. Vol. 57 No. 2 pp.750-769, 2008.
2. Hamilton D.B., Walowit J.A., Allen C.M. "A Theory of Lubrication by Microasperities", ASME J. Fluids Eng. Vol. 88 No. 1 pp.177-185, 1966.
3. Anno J.N., Walowit J.A., Allen C.M. "Microasperity Lubrication", ASME J. Tribol. Vol. 90 No. 2 pp.351-355, 1968.
4. Anno J.N., Walowit J.A., Allen C.M. "Load Support and leakage from Microasperity-Lubricated Face Seals", ASME J. Tribol. Vol. 91 No. 4 pp.726-731, 1969.
5. Tian H., Saka N., Suh N.P. "Boundary Lubrication Studies on Undulated Titanium Surface", Tribol. Trans. Vol. 32 No. 3 pp.289-296, 1989.
6. Tonder K. "Inlet Roughness Tribodevices: Dynamic Coefficients and Leakage", Tribol. Int. Vol. 34 No. 12 pp.847-852, 2001.
7. Han J., Fang L., Sun J.P., Ge S.R. "Hydrodynamic Lubrication of Microdimple Textured Surface Using Three-Dimensional CFD", Tribol. Trans. Vol. 53 No. 6 pp.860-870, 2010.
8. Greco A., Raphaelson S., Ehmann K., Wang Q., Lin C. "Surface Texturing of Tribological Interfaces Using the Vibromechanical Texturing Method", ASME J. Manuf. Sci. Eng. Vol. 131 No. 6 art no 061005, 2009.
9. Brinksmeier E., Riemer O., Twardy S. "Tribological behavior of microstructured surfaces for micro forming tools", Int J Mach Tool Manu, Vol. 50 No. 4 pp.425-430, 2010.
10. Graham E., Park C.I., Park S.S. "Fabrication of Micro-Dimpled Surfaces through Micro Ball End Milling", Int J Precis Eng Man, Vol. 14 No. 9 pp. 1637-1646, 2013.
11. Byun J.W., Shin H.S., Kwon M.H., Kim B.H., Chu C.N., "Surfac

DOI: XXX-XXX-XXXX

- 1  
2  
3 e texturing by micro ECM for friction reduction”, *Int J Precis*  
4 *Eng Man*, Vol. 11 No. 5 pp. 747-753, 2010  
5
- 6 12. Etsion I. “State of the Art in Laser Surface Texturing”, *ASME J*  
7 *Tribol* Vol. 127 No. 1 pp. 248-253, 2005.  
8
- 9 13. Etsion I., Burstein L. “A model for mechanical seals with regular  
10 microsurface structure”, *Tribol. Trans.* Vol. 39 No.3 pp. 677-683,  
11 1996.  
12
- 13 14. Etsion I., Halperin G. “A Laser Surface Textured Hydrostatic  
14 Mechanical Seal”, *Tribol. Trans.* Vol. 45 No. 3 pp. 430-434, 2002.  
15
- 16 15. Etsion I., Kligerman Y., Halperin G. “Analytical and  
17 Experimental Investigation of Laser-Textured Mechanical Seal  
18 Faces”, *Tribol. Trans.* Vol. 42 No. 3 pp. 511-516, 1999.  
19
- 20 16. Ronen A., Etsion I., Kligerman Y. “Friction-Reducing Surface-  
21 Texturing in Reciprocating Automotive Components”, *Tribol.*  
22 *Trans.* Vol. 44 No. 3 pp. 359-366, 2001.  
23
- 24 17. Ryk G., Kligerman Y., Etsion I. “Experimental Investigation of  
25 Laser Surface Texturing for Reciprocating Automotive  
26 Components”, *Tribol. Trans.* Vol. 45 No. 4 pp. 444-449, 2002.  
27
- 28 18. Brizmer V., Kligerman Y., Etsion, I. “A Laser Surface Textured  
29 Parallel Thrust Bearing”, *Tribol. Trans.* Vol. 46 No. 3 pp. 397-403,  
30 2003.  
31
- 32 19. Dekkers H.F.W., Duerinckx F., Szlufcik J., Nijs J. “Silicon  
33 surface texturing by reactive ion etching, *Opto-electronics*  
34 *Review*”, Vol. 8 No. 4 pp.311-316, 2000.  
35
- 36 20. Rui Z., Jian C., Kornel E., Chun X. “An Investigation on  
37 Deformation-based Surface Texturing”, *ASME J. Manuf. Sci.*  
38 *Eng.* Vol. 133 No.1 art no. 061017, 2011.  
39
- 40 21. Pettersson U., Jacobson S. “Tribological texturing of steel  
41 surfaces with a novel diamond embossing tool technique”, *Tribol.*  
42 *Int.* Vol. 39 No. 7 pp. 695–700, 2006.  
43
- 44 22. Pettersson U., Jacobson S. “Textured surfaces for improved  
45 lubrication at high pressure and low sliding speed of roller/piston  
46 in hydraulic motors”, *Tribol. Int.* Vol. 40 No.2 pp.355-359, 2007.  
47
- 48 23. Ma C.B., Zhu H., “An optimum design model for textured  
49 surface with elliptical-shape dimples under hydrodynamic  
50 lubrication”, *Tribol. Int.* Vol. 44 No. 9 pp. 987-995, 2011.  
51
- 52 24. Qiu M.F., Minson B., Raeymaekers, B. “The effect of texture  
53 shape on the friction coefficient and stiffness of gas-lubricated  
54 parallel slider bearings”, *Tribol. Int.* Vol. 67 pp. 278–288, 2013.  
55
- 56 25. Etsion I. “Improving tribological performance of mechanical  
57 components by laser surface texturing”, *Tribol. Lett.* Vol. 17 No.  
58 4 pp. 733-737, 2004.  
59
- 60 26. Xu X.Q., He S., Cai R.L. “Frictional characteristics of mechanical  
61 seals with a laser-textured seal surface”, *J. Mat. Proc. Tech.* Vol.  
62 129 No. 1 pp. 463-466, 2002.  
63  
64  
65